Hindawi
Advances in Civil Engineering
Volume 2019, Article ID 6040793, 9 pages
https://doi.org/10.1155/2019/6040793

Research Article

Field Test and Numerical Simulation of Dynamic Compaction of High Embankment Filled with Soil-Rock

Lu Zhang,[1] Guangqing Yang,[2] Dongliang Zhang,[1] Zhijie Wang,[2] and Jing Jin[3]

[1]*China State Construction Engineering Corporation Ltd., Beijing 100020, China*
[2]*School of Civil Engineering, Shijiazhuang Tiedao University, Shijiazhuang, Hebei 050043, China*
[3]*School of Civil Engineering, Hebei University of Science and Technology, Shijiazhuang, Hebei 050018, China*

Correspondence should be addressed to Jing Jin; jinjing@stdu.edu.cn

Received 27 June 2019; Accepted 22 August 2019; Published 10 September 2019

Academic Editor: Jian Ji

In view of the high filling height and large amount of soil and rock in the high-filled embankment, the variation law of the displacement field, stress field, and plastic zone of embankment body reinforced by dynamic compaction with different energy levels and the optimal compaction energy were analyzed by means of numerical simulations and field tests. Taking the embankment section of the Ping-Zan highway as an example, the construction scheme of dynamic compaction was designed, and the optimum tamping times and effective dynamic compaction depth of the embankment filled with soil-rock were obtained through the field test. The study showed that the displacement field and the stress field are redistributed after applying single-point compaction, and the volume of the shear plastic zone increases. The optimal number of slams for high-filled granular soil is 7 times, and the effective depth of dynamic compaction is 4.5 m. The result corresponds with that by the field test, which indicates that dynamic compaction is reasonable and has a significant effect on the high embankment filled with granular soil.

1. Introduction

Due to excellent mechanical properties, granular soils are used from ancient ages in different civil engineering applications, for example, earth and rockfill dams, highway and railway embankments, and landfills in dry or marine environment. Differential settlement would appear in a short time when construction had completed, with a weak bearing capacity or improper treatment to the foundation, which would affect the usage of the road or even reduce its service lifetime. The stability and settlement of an embankment or slope are always the most important points during the whole construction and service period [1, 2]. Strong tamping is to raise the large tonnage weight to a certain height and then fall freely. The ground is slammed repeatedly, giving the foundation impact and vibration, thus changing the physical properties of the soil, reducing the compressibility of the soil, and improving its bearing capacity. Practice has proved that the strong tamping method has a good effect on the reinforcement of granular soil, miscellaneous fill, cohesive soil, collapsible loess and other foundations, and prevention of liquefaction of silty soil and silt [3–5].

The reliability analysis of an engineering project is very important, in order to meet the requirements of settlement during construction and operation [6]. Since the first practical application of modern dynamic compaction techniques for ground treatment in 1965, many researchers have investigated the densification effects of dynamic compaction [7–11]. Modoni et al. [11] investigated the effects of compaction on the seismic performance of gravelly embankments. A number of test methods and numerical modeling have been performed to investigate the improvement parameters after compaction [12–15]. Ghanbari and Hamidi [14] studied four different slopes under impact loads of dynamic compaction which are modeled numerically using the finite element code ABAQUS. A constitutive model has been used successfully for simulation of dynamic compaction [16, 17].

Nowadays, the dynamic compaction method has been regarded as one of the most efficient techniques to ensure the

stability of gravelly soil backfill projects. When backfilled, gravelly soils are compacted circularly to achieve dense conditions and provide a sufficient bearing capacity. Hence, their mechanical behaviors should be understood. Poran et al. [18] used finite element calculation to obtain the stress response law of soil, the depth of impacts of slamming, and the development law of an equivalent plastic strain in the soil attack area. Taheri et al. [19] carried out a series of multiple-step loading tests and analyzed the strength and deformation characteristics of cement-mixed gravelly soils. Vallioppan et al. [20] applied the Fourier transform to study the vibration characteristics of vertical harmonic loads acting on the foundation surface and obtained the frequency domain solution of two-dimensional dynamic consolidation. When under compression or shear stress, larger grains are crushed into smaller grains. There are obvious changes in the grain size, grain shape, grain location, arrangement, and contact of gravelly soils [21]. The dynamic compaction characteristics of gravelly soils with a crushing effect have attracted increasing concern of scholars. Zou et al. [22] analyzed the monitoring results during compaction and the long period after compaction and compared with those from compaction by rolling. It is obvious that dynamic compaction has advantages such as a high degree of compaction and placement of a high-road embankment which is often required for construction of a highway in a mountain area. Wang et al. [23] investigated the relations between the grain crushing amount and the void ratio change of granular materials; the results showed that the higher the grain crushing amount is, the lower the void ratio of the sand is. Yao et al. [24] showed that a slamming impulse instead of slamming can be used as a parameter for strong tamping construction, and the calculation formula of the strong tamping range is derived, and the reinforcement formula is used to calculate and analyze the reinforcement range under strong tamping. The distribution characteristics of dry density of soil provide reference for similar projects in the future.

The dynamic compaction method is one of the most optimal techniques in gravelly soil backfill projects. However, the basic mechanical characteristics of gravelly soils and mechanisms of dynamic compaction have not yet been precisely determined. At present, the design of reinforcement of the soil-rock mixed embankment by dynamic compaction is generally empirical or semiempirical. In engineering, according to the experience of dynamic compaction in the soft soil foundation treatment, the corresponding parameters are designed. At present, the relevant industry standards of the Ministry of Transportation also lack the construction parameters and evaluation methods of the dynamic compaction method for the high embankment filled with granular soil. In this study, numerical simulation and field test methods are used to study the deformation of the high-filled granular soil embankment under the action of strong compaction in the Ping-Zan highway, Yuanshi County, Shijiazhuang City, Hebei Province. The foundation treatment project provides engineering practical experience and theoretical support.

2. Engineering Situation of Test Section

The main line of the Ping-Zan highway (Shitaibei-Zanhuang Section of Beijing–Kunming highway) in the Taihang Mountains of Hebei Province is 85.25 kilometers long, as shown in Figure 1. The highway construction of bi-directional and four-lane is adopted, and the design speed is 120 km/h. Along the highway, there are many high fill embankment sections along the gully, steep valley slope, and complex and changeable geology. The engineering geological characteristics of the test section K39 + 130~K39 + 150 are Archaean gneisses, mainly composed of biotite-plagioclase gneiss, amphibole gneiss, shallow granulites, amphibole, and marble. The Archaean metamorphic rocks in this area are generally characterized by large thickness, varied lithofacies, and widespread granitic gneiss lithology. Granitic gneisses generally belong to hard rocks.

The embankment is filled with abandoned excavation blasting of cutting slopes in adjacent sections. The filling is bad gradation gravel, according to the test results of the particle gradation curve. The maximum dry density of the filler is 2.21 g/cm^3, and the optimum moisture content is 6.2%.

3. Test Scheme of Dynamic Consolidation

According to the specific characteristics of the project and the engineering geological conditions, the tamping hammer spacing is 6.0 mm and the triangle arrangement is adopted. When the tamping energy is high, local compaction is used and tamped twice. When the tamping energy is low, full compaction is used and tamped once. In this project, the highest tamping energy is 2000 kN·m. The arrangement of the tamping points is shown in Figure 2.

4. Field Test Results Analysis

The rationality of dynamic compaction scheme should be evaluated according to the tamping effect. In this highway section, the settlement and dynamic stress of dynamic compaction are monitored on site.

4.1. The Settlement of Dynamic Compaction. In order to determine the optimum tamping times, 10 tamping points were selected in the test section for the tamping test, and the observation and record of tamping settlement were performed. Using the tamping times as x-coordinate and the tamping settlement as y-coordinate, the linear chart is drawn, as shown in Figure 3.

It can be seen from Figure 3 that the single tamping settlement reaches the maximum at the first tamping and then the single settlement gradually decreases with the increase of tamping times. It can be seen that the tamping times should be controlled within a reasonable range. The effect of dynamic compaction increases with the increase of tamping times; however, when the tamping times reaches a certain value, the effect of dynamic tamping is no longer significant by increasing the number of tamping. Under the tamping energy of 2000 kN·m, the single tamping settlement

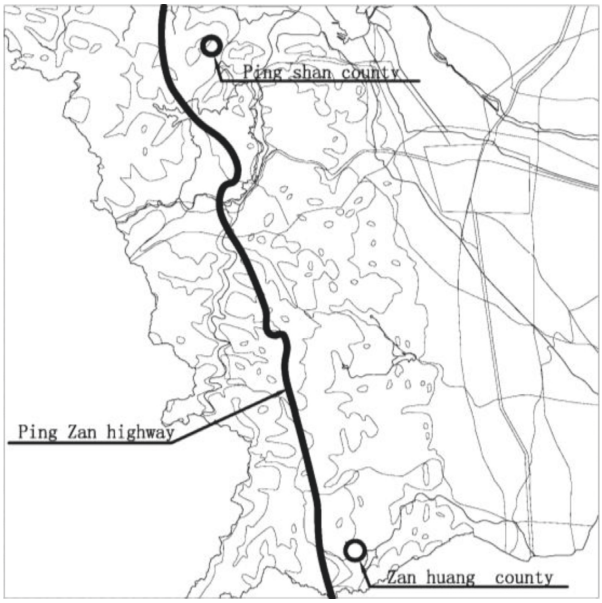

Figure 1: The route of the Ping-Zan highway.

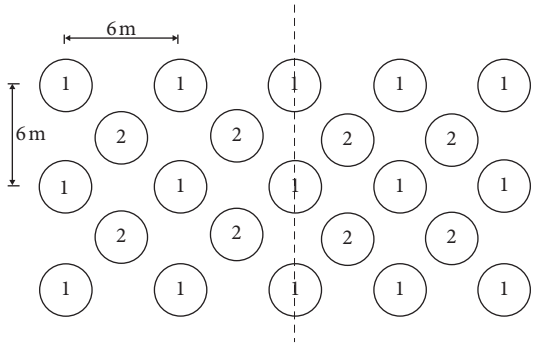

Figure 2: The tamping point floor plan.

of dynamic compaction after the 7th tamping is less than 50 mm. According to the Technical Specifications for Building Foundation Treatment, when the tamping energy is less than 4000 kN·m in practical engineering, the average settlement of the last two tamping is less than 50 mm, which is the best tamping times. From the relationship curve between the tamping settlement and the tamping times shown in Figure 3, it can be concluded that the 7th tamping time meets the effect of dynamic compaction.

4.2. The Dynamic Stress of Dynamic Compaction. In the Ping-Zan test section, the distribution curve of the dynamic stress range along vertical and horizontal directions is drawn, as shown in Figure 4. It can be seen that the dynamic stress of dynamic compaction is the largest under the rammer and decreases gradually with the increase of depth. The dynamic stresses are 58 kPa, 35 kPa, and 23 kPa in 2.0 m, 3.0 m, and 4.0 m below the rammer, respectively. The dynamic stress decreases by 39.7% and 34.3% from 2.0 m to 3.0 m and from 3.0 m to 4.0 m under the rammer, respectively. That is to say, the dynamic stress decreases gradually with the increase of the depth.

At the same depth under the rammer, the dynamic stress decreases gradually with the increase of the transverse

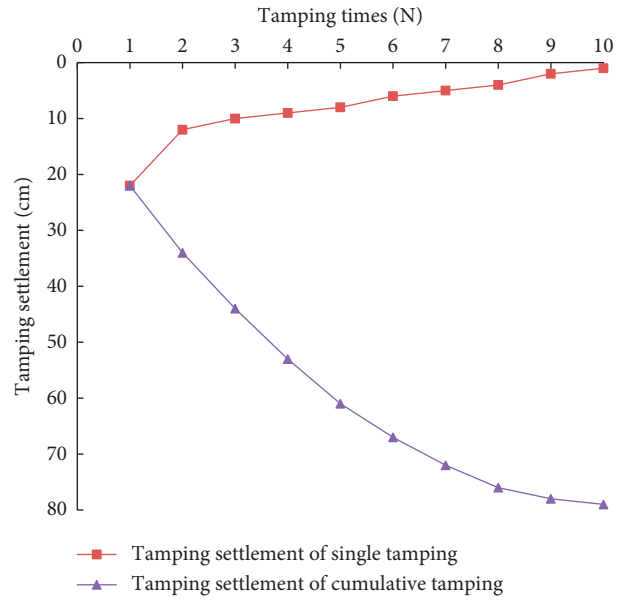

Figure 3: The relationship between tamping settlement and tamping times.

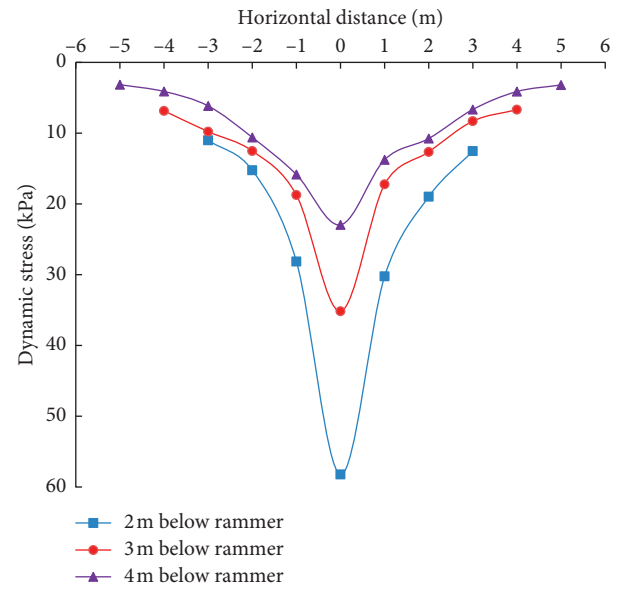

Figure 4: The distribution of the dynamic stress.

distance, but the attenuation amplitude slows down. The dynamic stress is basically above 10 kPa within 3 m from the center of the tamper, and the value of the dynamic stress is significantly reduced when the distance is greater than 3 m. It is concluded that the transverse effective reinforcement width of dynamic compaction is about 3 m. In design and construction, in order to achieve better reinforcement effect of dynamic compaction, the spacing of tamping points should not be too large.

5. Numerical Analysis of Dynamic Compaction

There are many factors affecting dynamic consolidation, and the stress-strain situation of soil is very complex. Therefore,

it is necessary to assume that the granular soil satisfies the following conditions: the embankment soil is a homogeneous isotropic elastoplastic semi-infinite space, the tamper is a rigid body, the influence of groundwater is neglected, and the foundation outside the certain range of the rammer is small deformation.

5.1. Model Establishment. The model is established and meshed, according to the influence range of soil affected by dynamic compaction. The x-axis, y-axis, and z-axis of the model represent the length, width, and height, respectively. A three-dimensional numerical model of dynamic compaction hammer and embankment soil is established, as shown in Figure 5. In the model, the number of grid elements of embankment soil and rammer are 3432 and 57, respectively.

5.2. The Failure Criterion. The embankment is regarded as an ideal elastic-plastic body in the calculation, so the Mohr–Coulomb failure criterion is used to simulate the numerical calculation. The mechanical model is

$$f = \sigma_1 - \sigma_3 \frac{1 + \sin\varphi}{1 - \sin\varphi} + 2c\sqrt{\frac{1 + \sin\varphi}{1 - \sin\varphi}}, \quad (1)$$

where σ_1 is the maximum principal stress of soil, σ_3 is the minimum principal stress of soil, c is the soil cohesion, and φ is the soil friction angle.

5.3. The Calculation Parameter. Based on JTG E40-2007 highway geotechnical test rules, the embankment fillings are sampled and tested in laboratory. The physical and mechanical parameters of the fillings are shown in Table 1.

5.4. Impact Load Application. As for the change rule of the dynamic compaction impact stress, the measured results all show that the stress wave of dynamic compaction hammer acting on soil has only one peak, and there is no obvious second peak, and the action time is very short. The measured results of dynamic impact stress show that there is only one peak value of the stress wave of hammer acting on soil, no obvious second peak, and the action time is very short. The peak value of the impact stress can be simplified to a triangular impact load without considering the effect of damping on the dynamic response. The peak value of the impact stress can be calculated to be 2.685 MPa.

Based on the established numerical calculation model, the drop distance of the rammer in the test section is 15 m under the tamping energy of 2000 kN·m. According to the field test, the action time of the impact stress is 0.1 s, as shown in Figure 6.

5.5. Numerical Simulation Results

5.5.1. Initial Ground Stress. The initial stress state of soil only under gravity is considered, as shown in Figure 7.

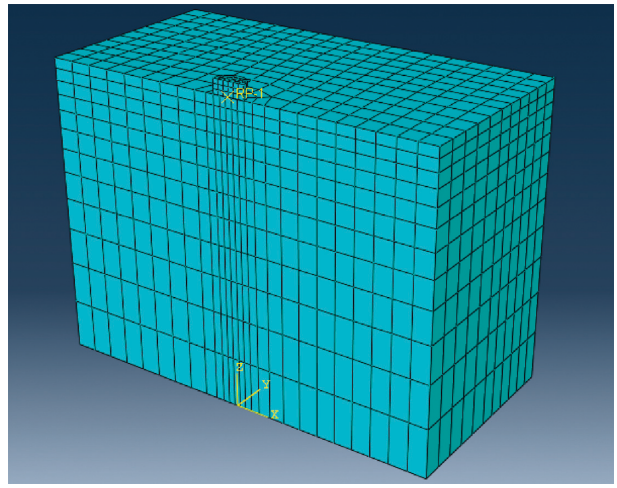

Figure 5: Three-dimensional numerical model diagram.

Table 1: The physical and mechanical parameters of the filling.

Density (kg/m^3)	Elastic modulus (MPa)	Poisson's ratio	Cohesion (kPa)	Internal friction angle (°)
2500	38	0.29	5	33

5.5.2. The Simulation of the Dynamic Compaction Effect. The height, depth, and depth of the subgrade are 15 m, 25 m, and 20 m, respectively. Through numerical simulation, the effect of dynamic compaction is evaluated by comparing the postconstruction settlement of the uncompacted embankment and compacted embankment. The displacement nephogram of the uncompacted embankment is shown in Figure 8, and the displacement nephogram of dynamic compaction under the tamping energy of 2000 kN·m is shown in Figure 9.

According to the above figure, the variation curve of settlement during the traffic-operating period is drawn, as shown in Figure 10. It can be seen that the effect of dynamic compaction is obvious, and the postconstruction settlement is obviously reduced.

5.5.3. Displacement Field Analysis. Vibration response of the high embankment is produced under the impact of the dynamic compaction wave. In this paper, only the vertical displacement response of the embankment is studied because dynamic compaction had an obvious effect on the vertical compaction of the embankment.

Figure 11 is a typical vertical displacement cloud diagram. It can be seen from the figure that the kinetic energy of the hammer is instantaneously transformed into the vibration wave to the soil during the construction of the hammer, which reduces the porosity of the soil and improves the compactness. Therefore, the deformation performance of the soil is improved, and the bearing capacity of the foundation is also improved. At the first strike of dynamic compaction, the vertical settlement of the embankment is relatively large. With the increase of the number of tamping, although the cumulative settlement

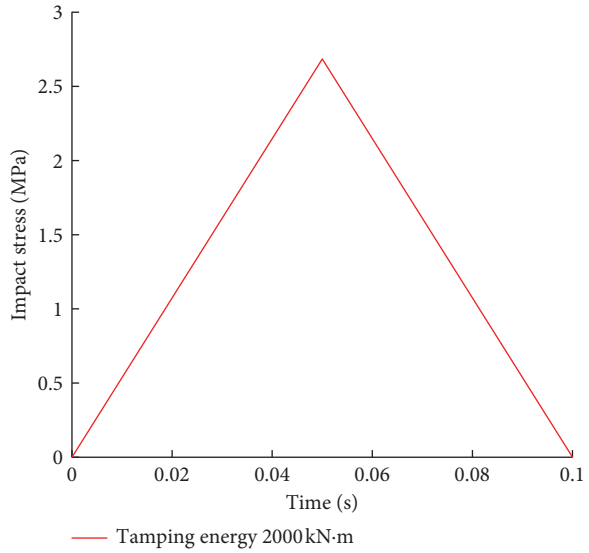

Figure 6: The impact load form.

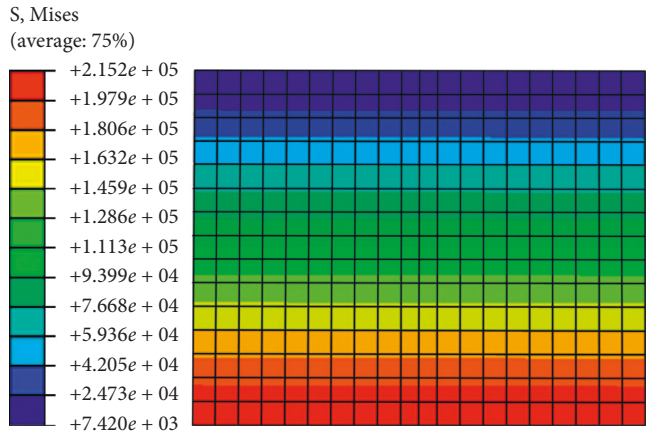

Figure 7: Initial stress cloud map.

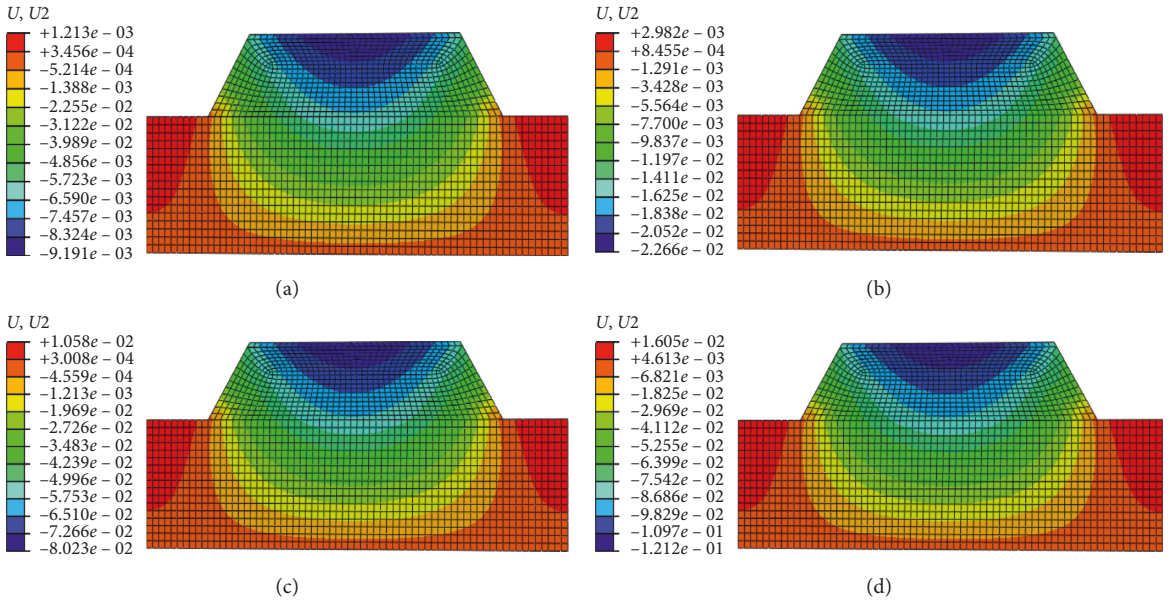

Figure 8: The postconstruction settlement of the uncompacted embankment (unit: m). (a) Settlement at the completion of filling. (b) Settlement after 1 year of operation. (c) Settlement after 5 years of operation. (d) Settlement after 10 years of operation.

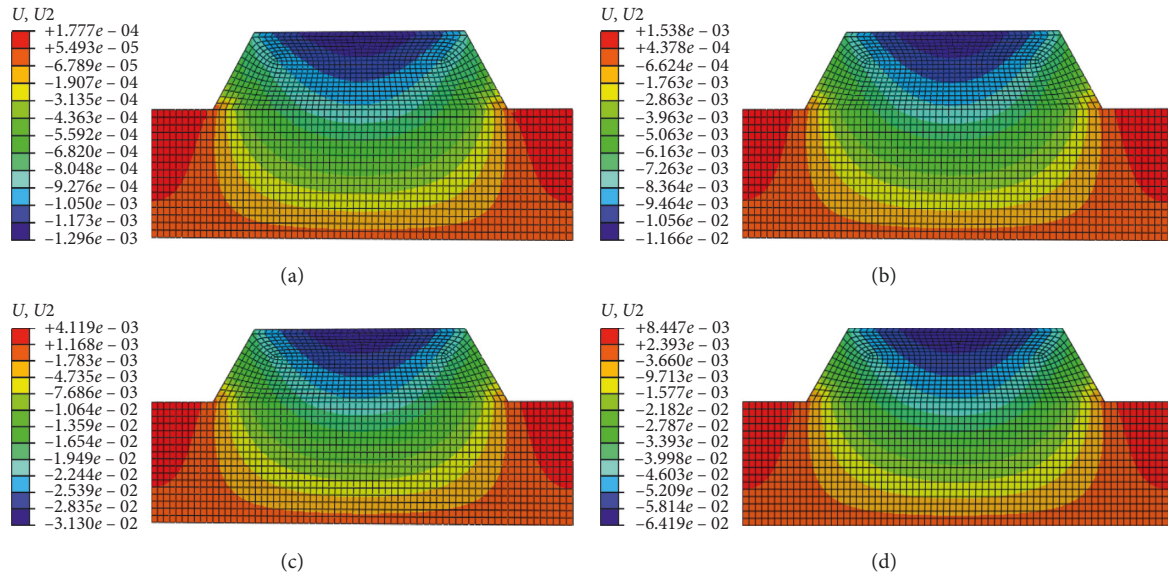

Figure 9: The postconstruction settlement of the compacted embankment (unit: m). (a) Settlement at the completion of filling. (b) Settlement after 1 year of operation. (c) Settlement after 5 years of operation. (d) Settlement after 10 years of operation.

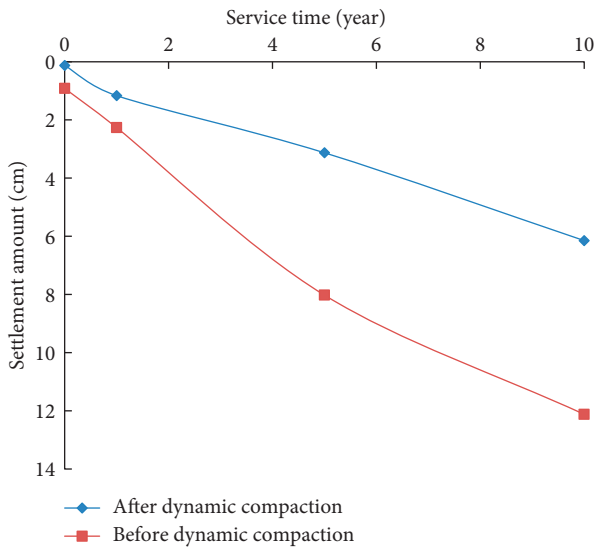

Figure 10: The postconstruction settlement with changes in service time.

increases gradually, the single-strike settlement decreases gradually and tends to be stable. During the seventh strike, the settlement of single tamping reached 4 cm. Tamping can stop when the click settlement is less than 50 mm, according to the Technical Specifications for Building Foundation Treatment (JGJ79-2012). Therefore, there is an optimum number of tamping in dynamic compaction construction. When the number of tamping is less than the optimum number of tamping, embankment filling can not be effectively strengthened. When the number of tamping is greater than the optimum number of tamping, resources will be wasted. Therefore, the optimum number of tamping in this project is 7 strikes.

5.5.4. Stress Field Analysis. Through the simulation of the impact load, the maximum principal stress nephogram in the process of tamping is obtained. Figure 12 shows the stress distribution nephogram of embankment filling at t_0 under the action of first, third, fifth, and seventh strikes.

From Figure 12, it can be seen that the stress circle presents an elliptical shape, and the embankment under the rammer is most impacted. The maximum principal stress decreases gradually with the increase of the depth from the center of the rammer, that is to say, the maximum principal stress appears on the interface between the rammer and the soil. With the increase of tamping times, the influence range of the maximum principal stress also increases until it becomes stable. In addition, the soil at the edge of the rammer appears to be uplifted.

5.5.5. Plastic Zone Analysis. During dynamic compaction, the impact of the hammer on the embankment can cause the displacement and shear of the soil particles, which results in rearrangement of the particles and plastic deformation of the soil due to dynamic compaction. In order to further study the effect of strong tamping reinforcement, the plastic zone range under the slamming action of 2000 kN·m energy level is analyzed, as shown in Figure 13.

As can be seen from the figure, the plastic development zone of dynamic compaction is an elliptical shape. Moreover, the plastic deformation zone of soil will continue to expand with the increase of tamping times. At the beginning, the increase in the range is more obvious and then gradually tends to stability. In the simulation process, the area with a plastic strain greater than 1% is considered as the effective depth area of dynamic consolidation; thus, the effective reinforcement depth of this dynamic compaction is 4.5 m.

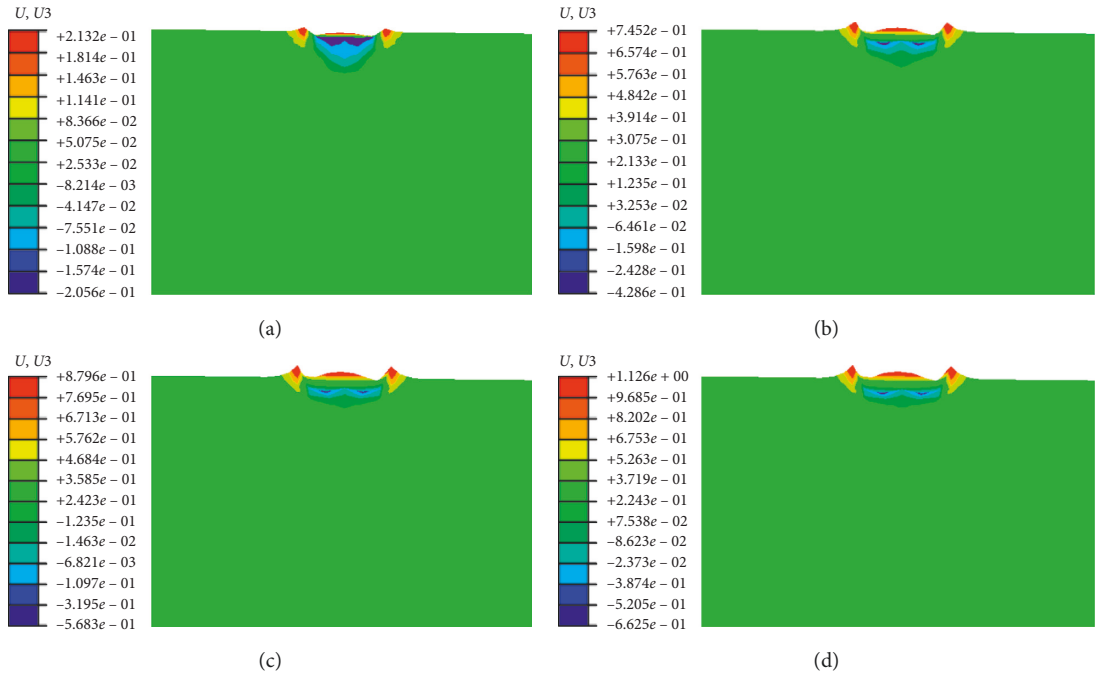

Figure 11: Vertical displacement cloud map (unit: m). (a) First strike. (b) Third strikes. (c) Fifth strikes. (d) Seventh strikes.

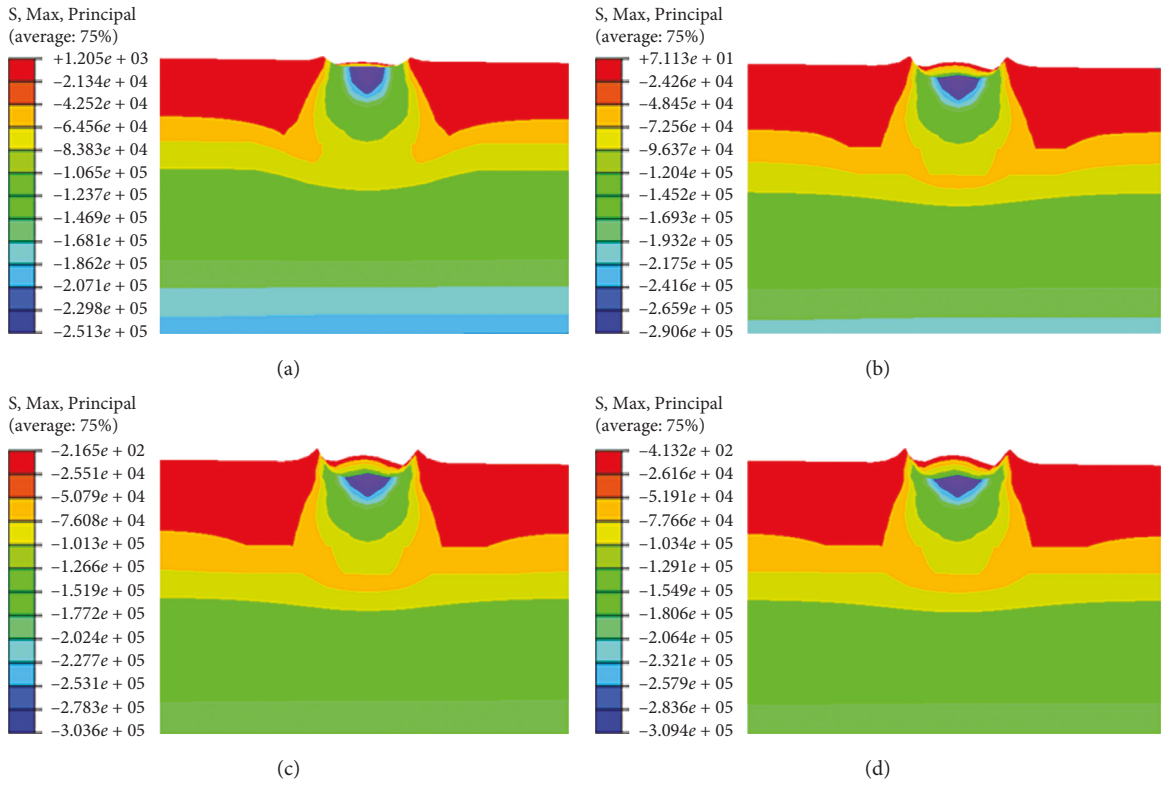

Figure 12: Maximum principal stress cloud. (a) First strike. (b) Third strikes. (c) Fifth strikes. (d) Seventh strikes.

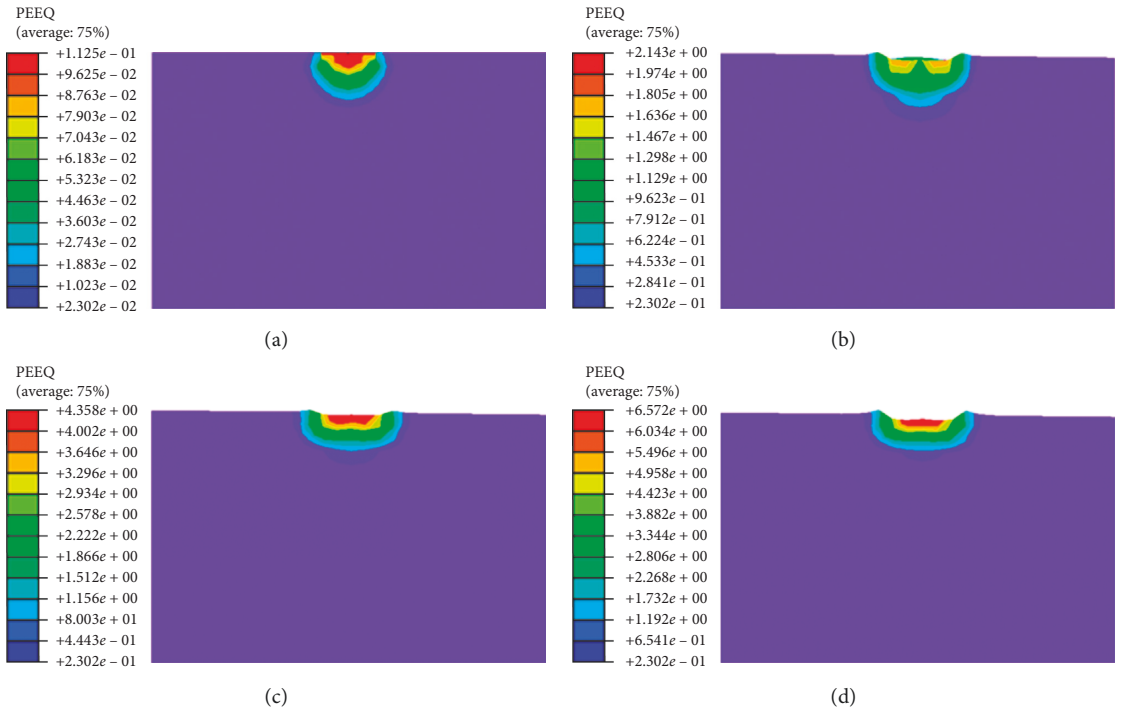

Figure 13: Equivalent plastic strain cloud. (a) First strike. (b) Third strikes. (c) Fifth strikes. (d) Seventh strikes.

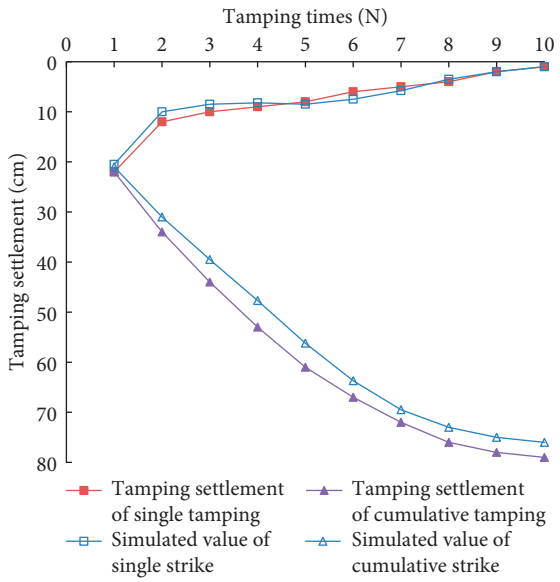

Figure 14: Comparison of field measured data and simulation test results.

6. Comparison of the Field Test with Numerical Simulation

It can be seen from Figure 14 that the simulation results are compared with the curves obtained from the field test data, and the soil displacements are relatively close and the deformation trend is the same. Other simulation results also conform to the law, indicating that the establishment of the model, the selection of parameters, and the calculation are reasonable. The calculation results can reflect the general law of dynamic compaction on high-filled granular soil. Since the actual project is affected by the surrounding environment, the superposition of hammers and construction machinery, the numerical simulation calculation value is slightly smaller than the field measured value.

7. Conclusion

The following conclusions may be drawn from this paper.

The simulation results basically coincide with those of the field results, which show that the establishment of the model, the design scheme, and the engineering parameters of dynamic compaction are reasonable.

The measured sag and dynamic stress results show that the optimum tamping times is 7 times, and the effective tamping reinforcement width is 4.5 m.

Placement of a high embankment is often required for construction of a highway in a mountain area. The results of the displacement field, stress field, and plastic zone analysis show that the dynamic compaction is suitable for a high embankment filled with soil-rock.

Dynamic compaction applied to a high embankment filled with soil-rock on the Ping-Zan highway made a successful example.

Data Availability

The simulation data and the model size data that were used to support the findings of this study are included within this article.

Conflicts of Interest

The authors declare that there are no conflicts of interest regarding the publication of this paper.

Acknowledgments

This study was supported by the National Natural Science Foundation of China (Grant nos. 51378322, 51709175), Hebei Province Natural Science Foundation (Grant nos. E2019208159, E2018210097), and Subsidized Project of Innovation Team Leading Talents Cultivation Program of Higher Education Institutions in Hebei Province (Grant no. LJRC023). All supports are very gratefully acknowledged.

References

[1] F. Zhang, Y. F. Gao, Y. X. Wu, and N. Zhang, "Upper-bound solutions for face stability of circular tunnels in undrained clays," *Géotechnique*, vol. 68, no. 1, pp. 76–85, 2018.

[2] J. Ji, C. Zhang, Y. Gao, and J. Kodikara, "Effect of 2D spatial variability on slope reliability: a simplified FORM analysis," *Geoscience Frontiers*, vol. 9, no. 6, pp. 1631–1638, 2018.

[3] A. A. Araei, H. R. Razeghi, S. H. Tabatabaei et al., "Loading frequency effect on stiffness, damping and cyclic strength of modeled rockfill materials," *Soil Dynamics & Earthquake Engineering*, vol. 33, no. 1, pp. 1–18, 2012.

[4] D.-V. Moldovan, A.-C. Nagy, L.-E. Muntean, and M. Ciotlaus, "Study on the stability of a road fill embankment," *Procedia Engineering*, vol. 181, pp. 60–67, 2017.

[5] K. Bouzelha, H. Hammoum, C. Amirouche, and T. Chaouadi, "Reliability analysis of stability to sliding of earthen embankment under seismic effect," *Procedia Structural Integrity*, vol. 5, pp. 77–84, 2017.

[6] J. Ji, C. Zhang, Y. Gao, and J. Kodikara, "Reliability-based design for geotechnical engineering: an inverse FORM approach for practice," *Computers and Geotechnics*, vol. 111, pp. 22–29, 2019.

[7] C. M. O. Nwaiwu, I. B. K. Alkali, and U. A. Ahmed, "Properties of ironstone lateritic gravels in relation to gravel road pavement construction," *Geotechnical and Geological Engineering*, vol. 24, no. 2, pp. 283–298, 2006.

[8] D. R. Biswal, U. C. Sahoo, and S. R. Dash, "Characterization of granular lateritic soils as pavement material," *Transportation Geotechnics*, vol. 6, pp. 108–122, 2016.

[9] P. S. Lin, C. W. Chang, and W. J. Chang, "Characterization of liquefaction resistance in gravelly soil: large hammer penetration test and shear wave velocity approach," *Soil Dynamics & Earthquake Engineering*, vol. 24, no. 9-10, pp. 675–687, 2004.

[10] Z. Cao, T. Leslie Youd, and X. Yuan, "Gravelly soils that liquefied during 2008 Wenchuan, China earthquake, M_s = 8.0," *Soil Dynamics and Earthquake Engineering*, vol. 31, no. 8, pp. 1132–1143, 2011.

[11] G. Modoni, M. Albano, E. Salvatore, and J. Koseki, "Effects of compaction on the seismic performance of embankments built with gravel," *Soil Dynamics and Earthquake Engineering*, vol. 106, pp. 231–242, 2018.

[12] E. Ghanbari and A. Hamidi, "Numerical modeling of rapid impact compaction in loose sands," *Geomechanics and Engineering*, vol. 6, no. 5, pp. 487–502, 2014.

[13] A. Ghassemi, A. Pak, and H. Shahir, "Numerical study of the coupled hydro-mechanical effects in dynamic compaction of saturated granular soils," *Computers and Geotechnics*, vol. 37, no. 1-2, pp. 10–24, 2010.

[14] E. Ghanbari and A. Hamidi, "Improvement parameters in dynamic compaction adjacent to the slopes," *Journal of Rock Mechanics and Geotechnical Engineering*, vol. 7, no. 2, pp. 233–236, 2015.

[15] D. Zekkos, M. Kabalan, and M. Flanagan, "Lessons learned from case histories of dynamic compaction at municipal solid waste sites," *Journal of Geotechnical and Geoenvironmental Engineering*, vol. 139, no. 5, pp. 735–751, 2013.

[16] T. Matsui and K.-C. San, "Finite element slope stability analysis by shear strength reduction technique," *Soils and Foundations*, vol. 32, no. 1, pp. 59–70, 1992.

[17] T. Triantafyllidis and I. Kimmig, "A simplified model for vibro compaction of granular soils," *Soil Dynamics and Earthquake Engineering*, vol. 122, pp. 261–273, 2019.

[18] C. J. Proan and J. A. Rodriguez, "Finite element analysis of impact behavior of sand," *Journal of the Japanese Society of Soil Mechanics & Foundation Engineering*, vol. 32, no. 4, pp. 81–92, 1992.

[19] A. Taheri, Y. Sasaki, F. Tatsuoka, and K. Watanabe, "Strength and deformation characteristics of cement-mixed gravelly soil in multiple-step triaxial compression," *Soils and Foundations*, vol. 52, no. 1, pp. 126–145, 2012.

[20] S. Valliappan, J. T. Yazdi, and C. Zhao, "Analytical solution for two-dimensional dynamic consolidation in frequency domain," *International Journal for Numerical and Analytical Methods in Geomechanics*, vol. 19, no. 10, pp. 663–682, 1995.

[21] F. A. Chuhan, A. Kjeldstad, K. Bjørlykke, and K. Høeg, "Porosity loss in sand by grain crushing-experimental evidence and relevance to reservoir quality," *Marine and Petroleum Geology*, vol. 19, no. 1, pp. 39–53, 2002.

[22] W.-L. Zou, Z. Wang, and Z.-F. Yao, "Effect of dynamic compaction on placement of high-road embankment," *Journal of Performance of Constructed Facilities*, vol. 19, no. 4, pp. 316–323, 2005.

[23] Z. C. Wang, R. C. K. Wong, and L. P. Qiao, "Investigation on relations between grain crushing amount and void ratio change of granular materials in one-dimensional compression and creep tests," *Journal of Rock Mechanics and Geotechnical Engineering*, vol. 3, pp. 415–420, 2011.

[24] Y. P. Yao and B. Z. Zhang, "Study on the range of dynamic consolidation based on body strain," *Chinese Journal of Geotechnical Engineering*, vol. 37, no. 9, pp. 2663–2671, 2016.